Scripta Materialia 146 (2018) 267–271

Contents lists available at ScienceDirect

Scripta Materialia

journal homepage: www.elsevier.com/locate/scriptamat

Regular article

Cold sintering approach to fabrication of high rate performance binderless $LiFePO_4$ cathode with high volumetric capacity

Joo-Hwan Seo [a], Kris Verlinde [a], Jing Guo [a,b], Damoon Sohrabi Baba Heidary [a], Ramakrishnan Rajagopalan [c,e], Thomas E. Mallouk [d], Clive A. Randall [a,b,e,*]

[a] Department of Materials Science and Engineering, The Pennsylvania State University, University Park, PA 16802, USA
[b] Center for Dielectrics and Piezoelectrics, The Pennsylvania State University, University Park, PA 16802, USA
[c] Department of Engineering, The Pennsylvania State University, Dubois, PA 15801, USA
[d] Department of Chemistry, The Pennsylvania State University, University Park, PA 16802, USA
[e] Materials Research Institute, The Pennsylvania State University, University Park, PA 16802, USA

ARTICLE INFO

Article history:
Received 7 November 2017
Accepted 2 December 2017
Available online xxxx

Keywords:
Cold sintering process
Lithium iron phosphate
Electrode density
Volumetric capacity
Rate performance

ABSTRACT

The cold sintering process (CSP) is an attractive method for densifying ceramic-based materials by using a transient aqueous solution at low temperature under high pressure. CSP was applied to increase the volumetric capacity density of lithium iron phosphate ($LiFePO_4$, LFP) based cathodes by densifying the cathode structure directly formed on a current collector. The binderless LFP cathode had a density of ~2.42 g/cm^3 and was capable of being cycled even at the high current rate of 10C. The gravimetric and volumetric capacity of the cold sintered LFP at 10C were ~102 mAh/g and 247 mAh/cm^3, respectively.

After being commercialized in 1992 by SONY, Li-ion rechargeable batteries (LIBs) have become essential to meet energy storage demands for small portable electronic devices, such as cellular phones and laptops, as well as automotive applications [1,2]. However, methods to develop cathode materials that can address safety, cost, and volumetric energy density are still in great demand [3,4]. Among the various cathode materials, lithium iron phosphate ($LiFePO_4$, LFP) is rated very high for meeting the practical demands of portable power and automotive applications due to its high safety, low cost, and excellent capacity [5–8].

Although LFP has a high theoretical gravimetric capacity, due to its low intrinsic density (3.6 g/cm^3), the use of this cathode material is limited in applications that are space- or volume- limited [9–11]. Moreover, the fabrication method currently used for making these cathodes further decreases their volumetric capacity. Usually, cathode films are fabricated by tape casting, using a mixture of active material, conductive carbon, and polymer binder. Almost half of the total volume of the cathode layer is occupied by inactive materials that include binders and occluded pores [12]. Hence, there is significant room to improve the density, capacity and microstructure of the cathode layer by minimizing the porosity and decreasing the amount of inactive materials.

Recently, we developed the cold sintering process, a low temperature densification technology for fabricating dense ceramics and ceramic-based composites [13–15]. As many as 50 chemistries that encompass a wide range of ceramics and ceramic-based composites were found to be easily densified at low temperature (<300 °C) under uniaxial pressure [16,17]. In this novel process, an aqueous transient solution was employed to facilitate the consolidation through a mediated dissolution and reprecipitation process under pressure and temperature. In our previous study, we showed that the cold sintering process was useful for fabricating LFP-based composite cathodes with high volumetric capacity [18]. Highly densified composite cathode pellets of ~89% relative density with volumetric capacity as high as 340 mAh/cm^3 at 0.1C (1C = 170 mA/g) were achieved. While these results were very promising, in order to extend the use of these pellets as electrode materials, we needed to demonstrate that the cold sintering process can be extended to thin/thick films that include direct fabrication of sintered cathode material onto the current collector.

In this study, we demonstrated the cold sintering approach for densifying thin LFP tape-cast cathodes pressed onto aluminum current collectors. The electrochemical performance of the sintered cathodes showed very high volumetric capacity retention even at high rates (10C) and good cyclability. This paper describes the process and characterization of the fabricated cathodes in detail. At this time we note that a continuous process has not yet been developed in the CSP, but we foresee a future possibility for a roll-to-roll process that could be developed.

* Corresponding author at: Department of Materials Science and Engineering, The Pennsylvania State University, University Park, PA 16802, USA.
E-mail address: car4@psu.edu (C.A. Randall).

https://doi.org/10.1016/j.scriptamat.2017.12.005
1359-6462/

The LFP cathode green tape was fabricated by the tape casting method previously reported by our group [19]. LFP powder was purchased from MTI corporations. Carbon nanofiber (CNF) used as a conductive carbon was provided by Mitsubishi Materials Inc. Binder system materials, namely QPAC 40 (Empower Materials, Newark, DE, USA) and S-160 (Tape Casting Warehouse, Morrisville, PA, USA), were used as a vehicle and a plasticizer. Initially, LFP and CNF (94:6 by wt.) were ball milled together overnight in an ethanol dispersion. After drying the mixture, the slurry was prepared by mixing LFP/CNF, QPAC 40, methyl ethyl ketone (MEK) and S-160 in the mass ratio of 21.3:13.7:64.7:0.3. The slurry was stirred overnight, and the green tape was fabricated using a laboratory tape casting machine and a doctor blade. A silicone-coated polyethylene terephthalate tape was used as the substrate. After being dried at room temperature, the LFP tape was punched into ½" diameter circles and peeled off from the substrate to be used as a cathode. The binder burn-out heat treatment was performed at 250 °C for 1 h to decompose organic materials from the cathode tape. The burned-out cathodes were composed of 94 wt% active material and 6 wt% carbon fiber. The composite cathode film was then humidified in a glass beaker with deionized water vaporized on the heating plate controlled at 60 °C for 20 min. Cold sintering was then done by pressing the LFP/carbon composite layer along with thin aluminum foil for 10 min at 180 °C under 240 MPa using a laboratory platen hot press. The microstructure of the prepared cathode sample was characterized, and the electrochemical performance of the cathode was evaluated by doing half-cell measurements.

The density of the cold sintered cathode was calculated from the mass and volume of the electrode. The volume was determined by measuring the thickness and area of the electrode. We also used the theoretical densities of 3.6 g/cm^3 and 1.95 g/cm^3 for LFP and carbon fiber, respectively, in order to compute the relative density. The thickness and the microstructure of cold sintered samples were characterized by scanning electron microscope (FESEM, FEI, NanoSEM 630) and transmission electron microscopy (TEM, FEI Titan3 G2) with energy dispersive spectroscopy (EDS). The average thickness was calculated from the cross-sectional SEM images. The fractured cross-sectional samples were prepared by ion milling. The TEM specimens were prepared by a standard method that includes thinning, polishing, and milling. X-ray diffraction (PANalytical Empyrean XRD system) with Cu-Ka radiation at a scan rate of 0.026° was used to characterize the crystalline structure of the cold sintered cathodes. To evaluate the electrochemical performance, half cells were assembled using a 2032 coin cell with the cold sintered cathode as the working electrode and lithium foil as the reference and counter electrode, in an argon-filled glove box. A polymer separator (0.45 μm-thick polyvinylidene difluoride membrane, Amersham, Germany) soaked with the liquid electrolyte (1 M lithium hexafluorophosphate solution in ethylene carbonate and dimethyl carbonate (EC/DMC = v/v ratio 50/50), Sigma-Aldrich, CA) was used. An eight channel potentiostat (Arbin Instruments) was used to evaluate the electrochemical performance. The cell was tested within the range of 2.4–4.2 V vs. Li^+/Li at room temperature. The gravimetric and volumetric capacity of the cathode were calculated based on the total mass and volume of the cathode excluding the aluminum foil.

Fig. 1 illustrates the fabrication process of the cold sintered LFP-based cathode. A tape casting technique followed by a binder burn-out process was employed to prepare binder-free LFP/carbon composite cathodes with high volumetric capacity. A slurry for the tape casting method was prepared by mixing LFP as an active material, carbon nanofiber as a conductive agent, and polymers. To achieve a high volumetric capacity density in the LFP cathode film, the as-prepared binder-free LFP/carbon fiber composites were humidified and then densified through the cold sintering process under 240 MPa pressure at 180 °C for 10 min.

Images of LFP/CNF powders and cross-sectional images of a LFP based cold sintered cathode obtained by SEM are shown in Fig. 2a–d. It was observed that CNF were well dispersed with LFP powders as shown in Fig. 2a. The high extrinsic surface area of the CNF was expected to provide a continuous conducting pathway and decrease the electrode resistance [20,21]. Fig. 2b shows a cross-sectional image of cold-sintered densified LFP on the aluminum foil current collector. The average thickness and amount of active material in the cold sintered cathode were 33 μm and 8.0 mg/cm^2, respectively. Fig. 2c and d show a magnified cross-sectional image of the sintered electrode. We see a very dense compact layer of LFP with low porosity. The calculated cathode density was ~2.42 g/cm^3, which is almost ~70% of relative density. It should be noted that this value is significantly higher than the typical densities of $LiFePO_4$ based cathodes fabricated by conventional tape-casting methods, which are on the order of ~1.9 g/cm [3,22,23]. This highly densified structure of the ceramic composite with low porosity is a key advantage of cathodes fabricated by the cold sintering process. XRD patterns of cold sintered LFP cathodes were investigated to confirm the crystallinity and phase purity of the cold sintered cathode, as shown in Fig. 2e. We saw diffraction peaks coming from LFP, carbon, and aluminum foil, as indicated in the figure. XRD also showed that the cold sintered LFP is a pure phase, and there is no additional secondary phase formed during the cold sintering process.

The detailed microstructures of cold-sintered LFP cathodes were investigated by TEM. TEM and EDS mapping images of the cold sintered cathode are shown in Fig. 3. The various sized grains of LFP and strips of carbon nanofibers between the LFP grains are observed. EDS mapping

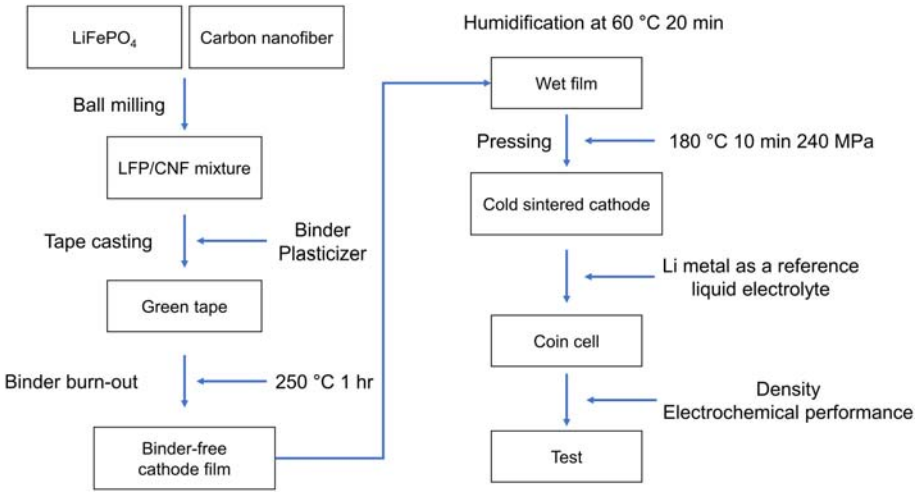

Fig. 1. A schematic diagram of the fabrication procedure for the LFP/CNF cathode composites using the cold sintering process.

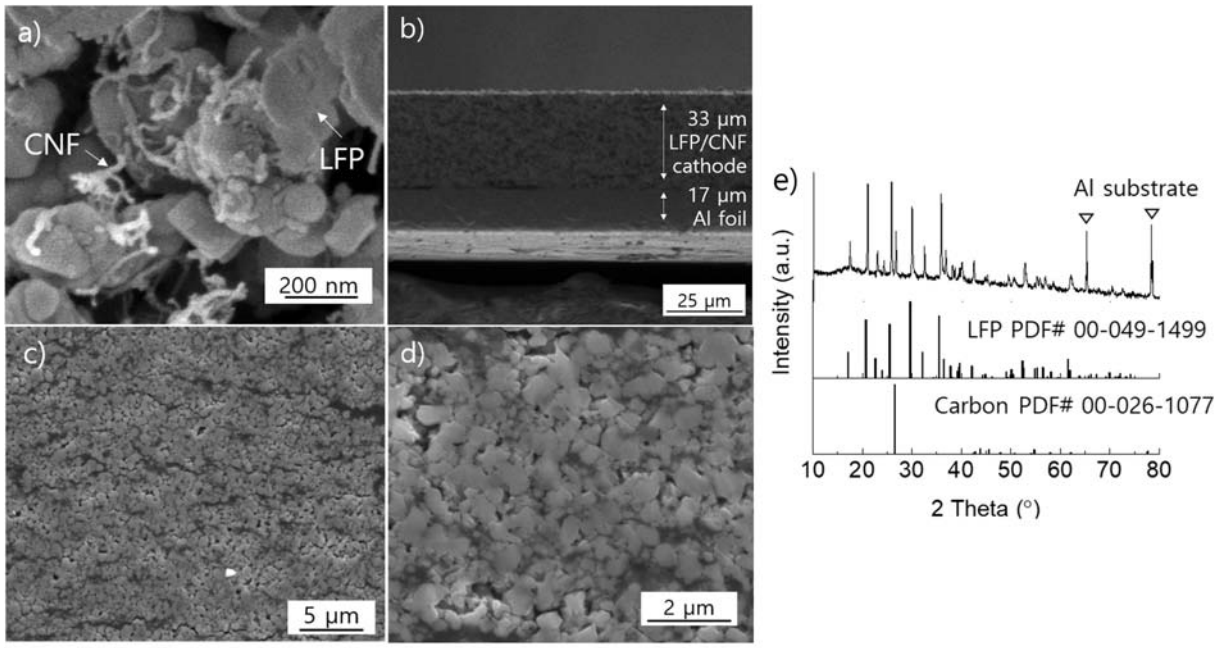

Fig. 2. SEM images of (a) ball milled mixture of LFP and CNF, (b–d) cross-sectional images of the cold sintered cathode at different magnifications and (e) a XRD pattern of a LFP cathode cold sintered with the XRD powder diffraction files (PDF) of LFP and carbon provided for reference.

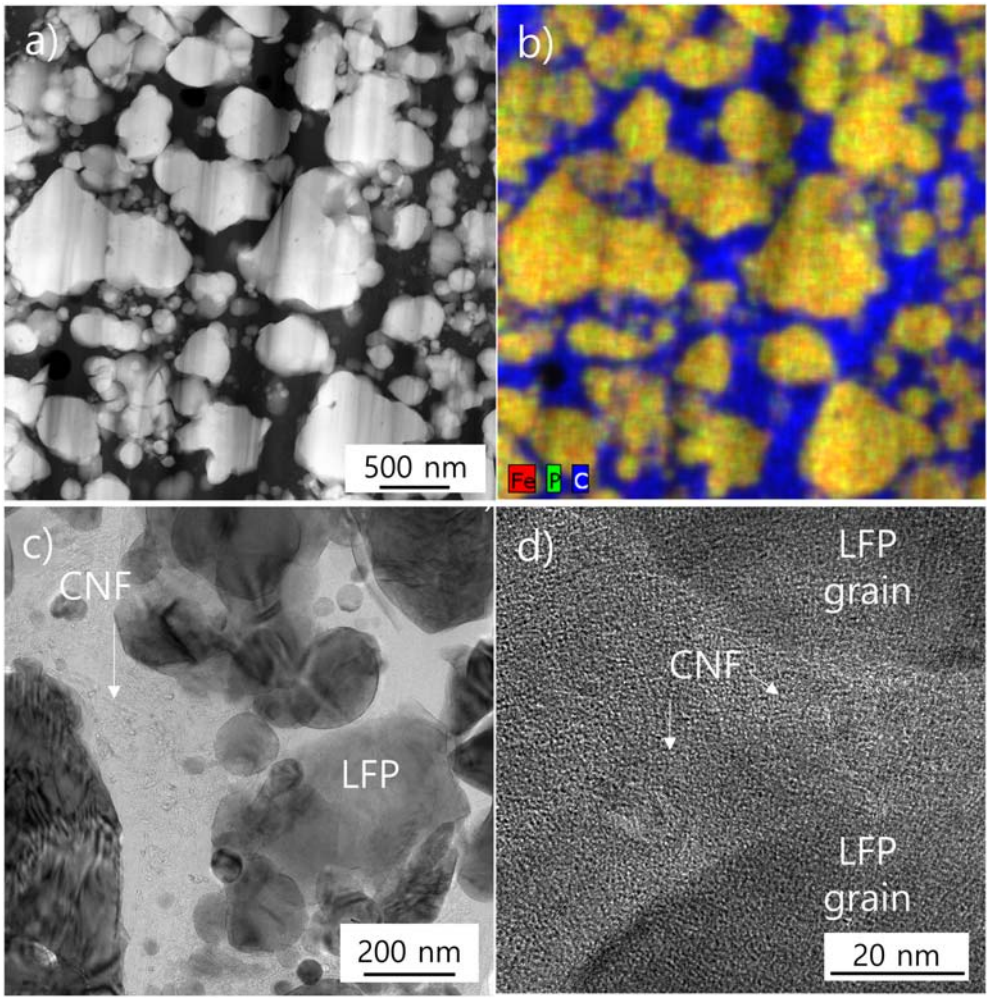

Fig. 3. TEM and EDS mapping images of cold-sintered LFP cathodes.

in Fig. 3b shows the distribution of LFP grains and carbon nanofibers, indicating that the carbon fibers are well dispersed between LFP grains. This interconnected structure of LFP by carbon nanofibers is expected to enhance efficient electron transfer in the cathode layer. As shown in Fig. 3c–d, clear grains and grain boundaries can be seen in the cathode. A small amount of an amorphous phase locates at the grain boundaries in some regions as reported in our previous paper. During the humidification process, a liquid phase can be formed, which leads to the densification of structures by a mediated dissolution-reprecipitation process. The re-precipitation can lead to an amorphous phase, epitaxial growth of primary grains, and precipitated nanograins, all in the grain boundaries of cold-sintered samples. It is also observed that the carbon nanofibers are located in the grain boundaries connecting the LFP grains. Therefore, it can be concluded that during cold sintering process, the dissolution and re-precipitation of LFP in amorphous grain boundaries results in a carbon fiber network structure.

The voltage profiles of a cold-sintered LFP cathode obtained at various current densities and their corresponding discharge capacities are shown in Fig. 4a. At all three current densities tested, the cold-sintered cathode showed flat voltage plateaus, indicating excellent charge transfer characteristics even at a discharge rate of 10C. At 0.1C, the cold sintered cathode had a gravimetric capacity of 154 mAh/g while the volumetric capacity was as high as 373 mAh/cm^3 as shown in Fig. 6b. This volumetric capacity of the cold sintered cathode is exceptionally higher than that of previously reported LFP-based cathodes, which are in the range of 159–227 mAh/cm^3 at similar C-rates of 0.04C-0.1C [5,12,22]. With an increase in charge/discharge rate to 10C, the cold sintered LFP cathode was still able to deliver a high gravimetric and volumetric capacity of ~102 mAh/g and 247 mAh/cm^3, respectively, which corresponds to a very short charge/discharge time of ~ 6 min. The capacity was fully recoverable when the C-rate was lowered to 1C. A comparison plot of gravimetric capacity of LFP-based cathodes as a function of C-rate was shown in Fig. 4c [10,24,25]. It is noted that the rate performance of the cold sintered cathode is quite competitive among those of previous reports even at high volumetric capacity density.

The cycling performance of the cold sintered cathode at high current rates of 1C and 10C was also investigated. As shown in Fig. 4c, the cold sintered cathode can deliver a very high capacity of ~127 mAh/g after 100 cycles with a high retention of initial capacity, over 90% at 1C. Even at the high rate of 10C, the cathodes also showed excellent retention of initial capacity, 93%. This means that the cold sintered cathode has high structural stability even though it is a highly densified binder-free composite structure [12,26]. Its excellent rate performance can be attributed to the densified binder-free structure of the cold sintered LFP/carbon composite. The densified structure increases the rate performance by minimizing the effects of resistive grain boundaries and facilitating fast electron transfer through the CNF network [27]. The process described above thus provides a path forward for fabricating adherent binderless cathodes directly on current collectors with high volumetric capacity.

In this study, we have succeeded in applying the cold sintering process to the fabrication of composite cathodes with high volumetric capacity, good rate performance, and cycling stability for large-scale Li-ion batteries. Using a binder burn-out procedure followed by the application of the cold sintering process, highly densified binder-free LFP/carbon composite cathodes were fabricated. SEM and TEM micrographs show clear evidence of cold sintering and densification. The density of the cold sintered LFP cathode was almost 70% of the theoretical density. The densified structured LFP cathodes exhibited very high gravimetric and volumetric capacity even at 10C rates. We believe that this unique processing is generic enough to be applied to other cathode and anode systems in order to improve both the volumetric capacity and rate capability of electrodes. Furthermore, with the earlier demonstration of Li-electrolytes such as LAGP and its composites being densified with cold

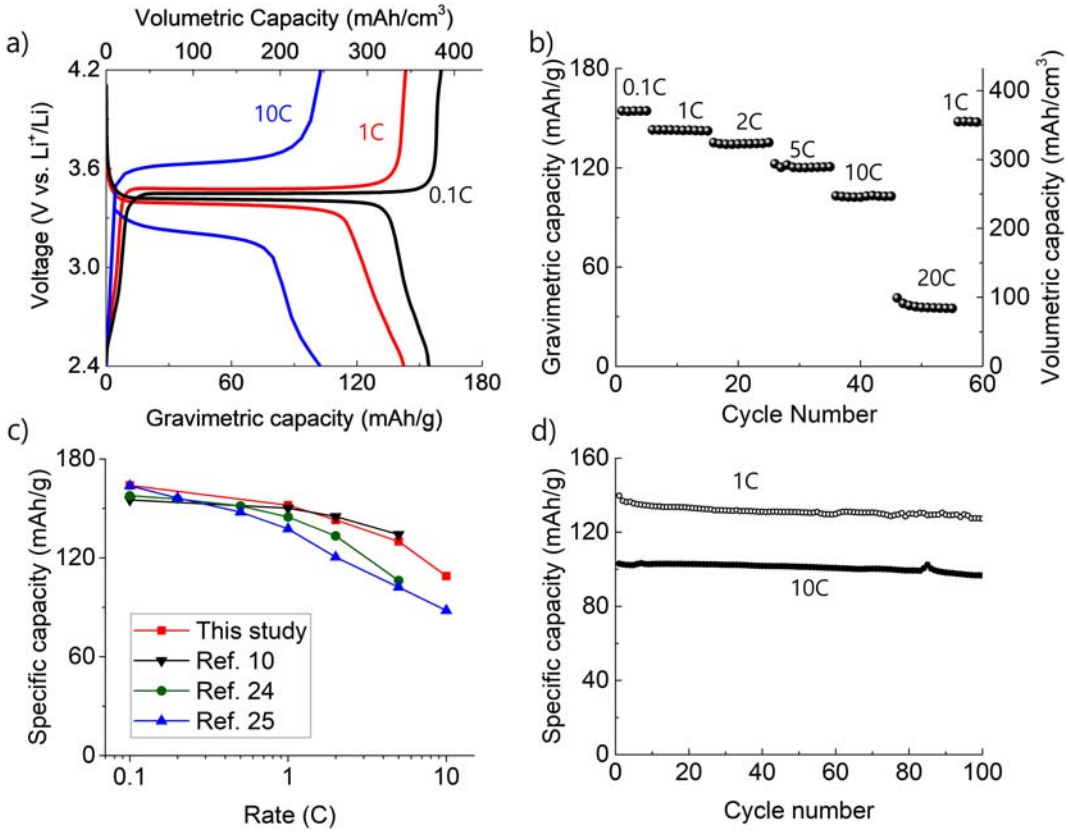

Fig. 4. (a) Voltage profiles of a cold sintered LFP cathode measured at various current densities, (b) gravimetric and volumetric capacities of a cold sintered LFP cathode at various C-rates, (c) comparison of rate characteristics of the cold sintered LFP-based cathode to those previously reported and (d) cycling performance of cold sintered LFP cathodes at different current densities.

sintering, there are also the possibility of co-processing a fully integrated solid-state Li-ion battery [28].

Acknowledgements

This work was supported by the Advanced Research Projects Agency within the U.S. Department of Energy under grant No. DE-AR0000766 to T. E. M., C. A. R., and J.-H. S., and also the National Science Foundation, as part of the Center for Dielectrics and Piezoelectrics under grant Nos. IIP-1361571 and 1361503 to K. B., J. G. and D. S. B. H. The authors would like to thank the MRI-MCL at The Pennsylvania State University for the use of characterization facilities.

References

[1] A.S. Arico, P. Bruce, B. Scrosati, J.-M. Tarascon, W.V. Schalkwijk, Nat. Mater. 4 (366) (2005).
[2] J. Wang, X. Sun, Energy Environ. Sci. 5 (2012) 5163.
[3] J. Chen, Dent. Mater. 6 (2013) 156.
[4] O.K. Park, Y. Cho, S. Lee, H.-C. Yoo, H.-K. Song, J. Cho, Energy Environ. Sci. 4 (2011) 1621.
[5] S.W. Oh, S.-T. Myung, H.J. Bang, C.S. Yoon, K. Amine, Y.-K. Sun, Electrochem. Solid-State Lett. 12 (2009) A181.
[6] S. Yang, Y. Song, P.Y. Zavalij, M.S. Whittingham, Electrochem. Commun. 4 (239) (2002).
[7] Y.-H. Huang, J.B. Goodenough, Chem. Mater. 20 (2008) 7237.
[8] T.V.S.L. Satyavani, A.S. Kumar, P.S.V.S. Rao, Eng. Sci. Technol. An. Int. J. 19 (2016) 178.
[9] Z. Li, D. Zhang, F. Yang, J. Amter. Sci. 44 (2009) 2435.
[10] C. Delacourt, P. Poizot, S. Levasseur, C. Masquelier, Electrochem. Solid-State Lett. 9 (2006) A352.
[11] S.-Y. Chung, J.T. Bloking, Y.-M. Chiang, Nat. Mater. 1 (2002) 123.
[12] X. Qin, X. Wang, J. Xie, L. Wen, L. J. Mater. Chem. 21 (2011) 12444.
[13] J. Guo, H. Guo, A.L. Baker, M.T. Lanagan, E.R. Kupp, G.L. Messing, C.A. Randall, Angew. Chem. Int. Ed. Eng. 55 (11457) (2016).
[14] J. Guo, S.S. Berbano, H. Guo, A.L. Baker, M.T. Lanagan, C.A. Randall, Adv. Funct. Mater. 26 (2016) 7115.
[15] S. Funahashi, J. Guo, H. Guo, K. Wang, A.L. Baker, K. Shiratsuyu, C.A. Randall, J. Am. Ceram. Soc. 100 (2017) 546.
[16] H. Guo, A. Baker, J. Guo, C.A. Randall, J. Am. Ceram. Soc. 99 (2016) 3489.
[17] A. Baker, H. Guo, J. Guo, C.A. Randall, J. Am. Ceram. Soc. 99 (2016) 3202.
[18] J.-H. Seo, J. Guo, H. Guo, K. Verlinde, D.S.B. Heidary, R. Rajagopalan, C.A. Randall, Ceram. Int. 43 (2017) 15370.
[19] L. Gao, S.-W. Ko, H. Guo, E. Hennig, C.A. Randall, J. Am. Ceram. Soc. 99 (2016) 2023.
[20] X.-L. Wu, Y.-G. Guo, J. Su, J.-W. Xiong, Y.L. Zhang, L.J. Wan, Adv. Energy Mater. 3 (2013) 1155.
[21] O. Toprakci, H.A.K. Toprakci, L. Ji, G. Xu, Z. Lin, X. Zhang, ACS Appl. Mater. Interfaces 4 (2012) 1273.
[22] K. Zaghib, J. Shim, A. Guerfi, P. Charest, K.A. Striebel, Electrochem. Solid-State Lett. 8 (A207) (2005).
[23] MTI corporation Online, http://www.mtixtl.com/Li-IonBatteryCathode-AluminumfoildoublesidecoatedbyLiFePO4241mm.aspx, (accessed October 2017).
[24] J.-H. Kim, S.C. Woo, M.-S. Park, K.J. Kim, T. Yim, J.-S. Kim, J. Power Sources 229 (2013) 190.
[25] J. Yang, J. Wang, Y. Tang, D. Wang, B. Xiao, X. Li, R. Li, G. Liang, T.-K. Sham, X. Sun, J. Mater. Chem. A 1 (7306) (2013).
[26] J. Chen, M.S. Whittingham, Electrochem. Commun. 8 (855) (2006).
[27] D. Xu, X. Chu, Y.-B. He, Z. Ding, B. Li, W. Han, H. Du, F. Kang, Electrochim. Acta 152 (2015) 398.
[28] S.S. Berbano, J. Guo, H. Guo, M.T. Lanagan, C.A. Randall, J. Am. Ceram. Soc. 100 (2017) 2123.